Hong Kong J Radiol. 2013;16:312-21 | DOI: 10.12809/hkjr1313183

PICTORIAL ESSAY

Sagittal Magnetic Resonance Imaging of the Brain: One Side of the Story

F Mubarak[1,2], D Lau[1], S Alam[2], AP Tan[1], PL Kei[1]

[1]Department of Diagnostic Radiology, Singapore General Hospital, Outram Road, Singapore 169608; and
[2]Department of Radiology, Aga Khan University Hospital, Karachi, Pakistan

ABSTRACT

Sagittal magnetic resonance imaging of the brain is included in many brain imaging protocols and, when taken alone, the sagittal plane is useful for providing diagnostic information about common pathologies. The sagittal plane is also a valuable time-efficient method for reviewing pertinent findings with clinicians. The purpose of this pictorial review was to revisit the normal anatomy and common pathologies that can be detected in sagittal magnetic resonance images of the brain.

Key Words: *Brain diseases; Magnetic resonance imaging*

中文摘要

大腦的磁共振矢狀位成像：故事的一面

F Mubarak, D Lau, S Alam, AP Tan, PL Kei

多數腦磁共振掃描方案都包含矢狀位成像。單獨憑借矢狀面圖像也能提供常見病症的診斷信息，所以非常有用。矢狀面成像亦是與臨床醫生共同評估疾病相關信息的一種有價值且頗節省時間的方法。本圖文回顧在大腦的磁共振矢狀位成像上可檢測到的正常解剖現象和常見病症。

INTRODUCTION

Sagittal magnetic resonance imaging (MRI) of the brain is included in many brain imaging protocols, but these images are often underutilised both by clinicians and radiologists. There is a lack of awareness of the importance of the sagittal imaging plane and the potential findings that could be easily detected by using sagittal plane MRI alone.

This pictorial review highlights the importance of understanding the anatomy of the brain on sagittal plane MRI, and the common pathologies that can be easily identified on the sagittal plane.

ANATOMY OF THE BRAIN IN THE SAGITTAL PLANE

The anatomy of the brain in the sagittal plane is shown in Figure 1. The corpus callosum is a large curved midline structure of commissural fibres. The corpus callosum connects the left and right cerebral hemispheres and facilitates interhemispheric communication.[1] The structure is divided into four parts,

Correspondence: *Dr PL Kei, Department of Diagnostic Radiology, Singapore General Hospital, Outram Road, Singapore 169608. Tel: (65) 6326 6203; Fax: (65) 6326 5242; Email: kei.pin.lin@sgh.com.sg*

Submitted: 8 Apr 2013; Accepted: 5 Sep 2013.

Figure 1. Normal anatomy of the brain on sagittal plane T1-weighted magnetic resonance image.
Abbreviations: A = corpus callosum; B = thalamus; C = pituitary gland; D = medulla; E = clivus; F = cerebellum; G = pineal gland; H = superior sagittal sinus; I = torcular herophili.

namely the rostrum, genu, body, and splenium. The corpus callosum lies below the lower free edge of the falx cerebri and forms the roof of the anterior horn of the lateral ventricles. The corpus callosum develops in an anterior-to-posterior pattern through interhemispheric midline fusion, with specialised midline glial guiding the callosal fibres to the other side. Development of the genu of the corpus callosum in the human embryo begins at around the eighth week of gestation. The interhemispheric crossing fibres begin to traverse the massa commissuralis in this region at the 11th to 12th weeks of gestation, progressing caudally, forming the body and the splenium. At 18 weeks of gestation, the splenium is thin and not fully developed, but the genu and body can be visualised clearly. The rostrum develops last at 18 to 20 weeks of gestation.[2] In sagittal plane MRI, the curved inverted U structure of the corpus callosum can be easily identified in the midline, beneath the cerebral cortex.

The hypothalamus and thalamus are located at the centre of the forebrain, just above the midbrain, and are bridged by a grey matter structure called the massa intermedia. The hypothalamus is responsible for a number of metabolic processes and control of the autonomic nervous system. The hypothalamus synthesises and secretes hypothalamic-releasing hormones, and regulates the secretion of the pituitary hormones. The hypothalamus controls thermoregulation, the sleep-wake cycle, and other circadian rhythms.[1]

The pituitary gland is the master gland that secretes nine pituitary hormones that regulate homeostasis. In sagittal plane MRI, the gland is bilobed and lies in the pituitary fossa. The gland has a shallow stalk, the infundibulum, and arises from the tuber cinereum in the floor of the third ventricle. The anterior lobe is adherent to the posterior lobe by a narrow zone called the pars intermedia. The anterior lobe of the pituitary gland is iso–signal intense to the grey matter of the brain, while the posterior lobe is hyperintense in fast spin echo T1-weighted (T1W) non-contrast images. The optic chiasm lies superior to the pituitary gland and, because of this, a mass arising from the pituitary often affects vision, causing bitemporal hemianopia. The sphenoid sinus lies beneath the pituitary fossa,[1] providing a natural pathway for neurosurgeons performing surgical resection of the pituitary mass.

The brain stem connects the cerebral hemispheres with the spinal cord. The brain stem provides the main motor and sensory innervation to the face and neck via the cranial nerves, and provides the conduction pathway between the brain and the rest of the body. The brain stem controls basic vital life functions such as heart rate, blood pressure, respiration, pain sensitivity, alertness, and consciousness. Injury to the brain stem thus has serious consequences.[1] The brainstem is bounded anteriorly by the clivus-basisphenoid above and the basi-occiput below. The brainstem is subdivided into the midbrain, pons and medulla, and these structures are easily appreciated in sagittal plane MRI. The part of the midbrain posterior to the aqueduct is known as the tectum or quadrigeminal plate, which is made up of four rounded prominences — the superior and inferior colliculi.

The cerebellum is a cauliflower-like structure that plays an important role in motor coordination and balance. The cerebellum is separated from the occipital lobe by the tentorium and is connected to the brain stem by three pairs of cerebellar peduncles — the superior, middle, and inferior cerebellar peduncles. On each side, below the middle cerebellar peduncle, is the flocculus, which extends laterally from the midline and lies close to the lateral recess and part of the choroid plexus found in the superior-lateral portion of the inferior horn of the fourth ventricle. The cerebellar tonsils are the most anterior and inferior part of the hemispheres[3] and are

best appreciated in sagittal plane imaging. In addition, the integrity of the cerebellar vermis can be visualised on sagittal plane images.

The pineal gland is a pine cone–shaped structure (hence its name) that lies between the posterior ends of the thalami and between the splenium of the corpus callosum and the superior colliculus. The gland is separated from the splenium of the corpus by the cerebral veins.[1]

The ventricular chains are four cerebrospinal fluid (CSF)–filled ependymal-lined cavities deep within the brain. These chains are paired lateral, and midline third and fourth ventricles. The chains communicate with each other and with the central canal of the spinal cord and subarachnoid space. The third ventricle communicates with the fourth ventricle via the cerebral aqueduct. The lateral ventricle contains the choroid plexuses, which are responsible for CSF production and, in turn, bathe and cushion the brain within their bony confines.[4]

The superior sagittal sinus occupies the attached convex margin of the falx cerebri and is the largest of the venous channels found between layers of dura mater in the brain. The sinus receives blood from internal and external veins of the brain, receives CSF from the subarachnoid space, and ultimately empties into the internal jugular vein. The straight sinuses, and the inferior sagittal and great cerebral (great vein of Galen) veins form the deep venous sinuses of the brain. All the sinuses drain posteriorly at a confluence called the torcula.[4]

BRAIN PATHOLOGIES IN THE SAGITTAL PLANE

Sagittal plane MRI is a very useful sequence for diagnosing different brain pathologies such as congenital malformations, infections, degenerative diseases, neoplasms, and vascular abnormalities. T1W images are good for identifying the anatomy, while T2W images are useful for identifying pathological states and the relationship between the CSF and the other brain structures.

Congenital Malformations

Chiari malformation (CM) is a congenital anomaly of the hindbrain, with a scale of severity ranging from I to IV, with type IV being the most severe. CM types III and IV are very rare. CM types I, II, and III involve varying degrees of herniation of rhombencephalic derivatives out of the posterior cranial fossa, while CM type IV involves cerebellar degeneration with no herniation of the hindbrain. CM types II, III, and IV are complex congenital malformations. CM types II, III, and IV are almost always associated with myelomeningocele, and involve the skull, dura, brain, spine, and spinal cord, with downward displacement of the medulla, fourth ventricle, and cerebellum into the cervical spinal canal. Elongation of the pons and fourth ventricle, probably due to a relatively small posterior fossa, are also present. CM type II is relatively common, with an incidence of 1 in 1000 live births. CM type II is associated with spina bifida and herniation of the vermis with descent of the rhombencephalon.[5] Unlike CM types II, III, and IV, CM type I often remains asymptomatic until adulthood, and occurs most commonly in women. The anomaly is characterised by herniation of the cerebellar tonsils through the foramen magnum into the cervical spinal canal, which can be best appreciated on MRI in the sagittal plane. The cerebellar tonsils are elongated in a peg-like fashion. Mild inferior extension causing kinking or flattening of the medulla may be seen. The reference line that is drawn across the basion to the opisthion defines the lower margin of the posterior cranial fossa, and is used as the reference for measuring tonsillar herniation. Syringohydromyelia (most commonly in the cervical spinal cord [Figure 2])

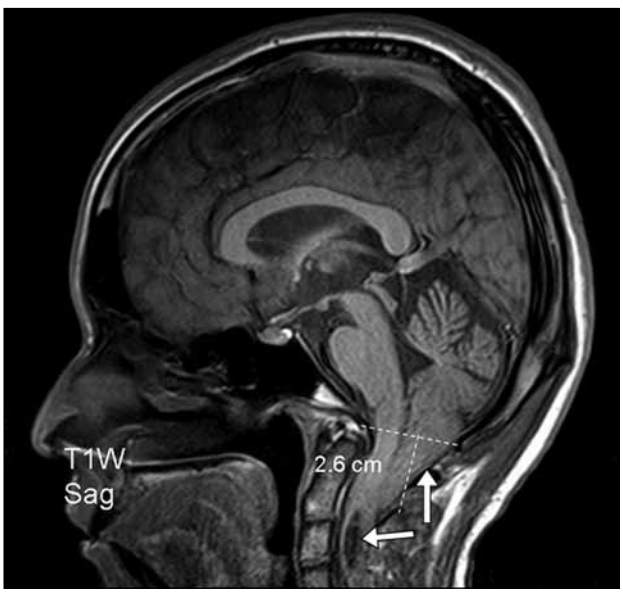

Figure 2. A sagittal plane T1-weighted magnetic resonance image of the brain of a 12-year-old boy with chronic headaches. The image shows the cerebellar tonsil herniated through the foramen magnum (vertical arrow), 2.6 cm below the dotted line, with cervical cord syrinx (horizontal arrow). This is associated with Chiari malformation type I.

is present in approximately 25% of patients with CM type I.[5]

Congenital aqueductal stenosis (AS) is a relatively common cause of obstructive hydrocephalus. Congenital AS can be inherited in an X-linked recessive manner, and therefore more often affects boys than girls. AS is one of the most common causes of foetal hydrocephalus. In addition, the adult form of AS can be acquired due to infection or any space-occupying lesion in the vicinity of the cerebral aqueduct.[6] On sagittal plane MRI, there is dilatation of the lateral and third ventricles and a normal-sized fourth ventricle, with or without dilatation of the upper, not lower, portion of the cerebral aqueduct (Figure 3). On phase-contrast MRI CSF flow studies, the absence of flow void at the aqueductal level indicated absence of CSF flow.[7]

Agenesis of the corpus callosum is another congenital malformation that is well appreciated on sagittal plane MRI. The anomaly may occur in isolation, or be associated with other central nervous system (CNS) or systemic malformations. The corpus callosum may be completely or partially absent in this anomaly. Complete agenesis usually occurs early in embryonic development, while partial agenesis occurs at a later gestational stage. In complete agenesis of the corpus callosum, sagittal plane T1W MRI of the brain shows complete absence of the corpus callosum. The cingulate sulcus is absent, and the medial hemispheric sulci reach the third ventricle in a radial fashion (Figure 4) with other associated abnormalities. In partial agenesis of the corpus callosum, the posterior genu and the anterior corpus callosum are present, while the posterior body, splenium, and rostrum are absent.[8]

Infections

There are some infectious processes that commonly involve the brain and are well appreciated on sagittal MRI. Tuberculous meningitis is the most common form of CNS tuberculosis, and is associated with high morbidity and mortality. The disease occurs when bacteria (*Mycobacterium tuberculosis*) invade the membranes and fluid surrounding the brain and spinal cord. The infection usually begins elsewhere in the body, often in the lungs, and may spread to the meninges by a variety of routes. Bacilli seeding to the meninges result in the formation of small subpial or subependymal foci of infection.[9] MRI features of

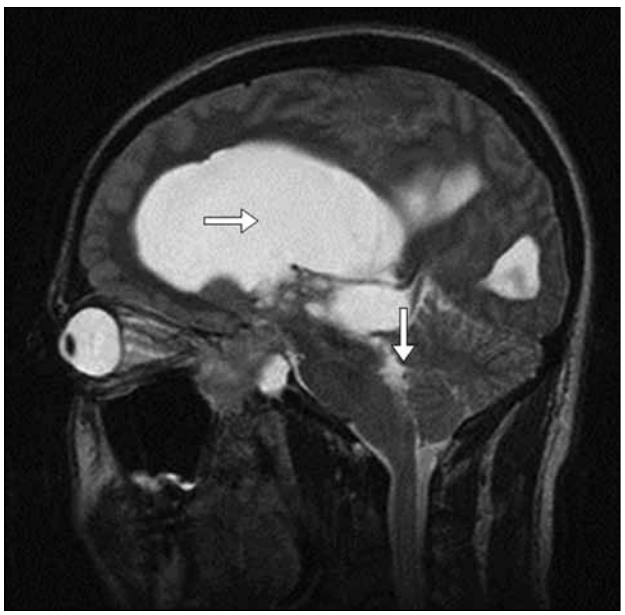

Figure 3. A sagittal plane T2-weighted magnetic resonance image of the brain of a 40-year-old woman with unresolving headaches. The image shows dilatation of the lateral and third ventricles (horizontal arrow) with a normal-sized fourth ventricle (vertical arrow), with dilatation of the cerebral aqueduct compatible with cerebral aqueductal stenosis. The cause is thought to be infection.

Figure 4. A sagittal plane post-contrast fluid-attenuated inversion recovery magnetic resonance image of the brain of a 1-year-old boy with developmental delay and tonic-clonic seizures. The image shows agenesis of the corpus callosum (vertical arrow) with schizencephaly (horizontal arrow). The thin arrow shows the cleft in the hemisphere communicating with the third ventricle, as seen radially in the sagittal plane.

tuberculomas depend on whether the lesion is non-caseating, caseating with a solid centre, or caseating with a liquid centre. On MRI (including the sagittal plane), non-caseating tuberculomas appear hypointense on T1W images and hyperintense on T2W images, with homogenous enhancement after contrast administration. Caseating tuberculomas with solid centres appear hypointense or isointense on both T1W and T2W images, with ring enhancement on contrast MRI. Tuberculomas with central liquefaction of the caseous material typically show central hypointensity on T1W images and hyperintensity on T2W images with ring enhancement after contrast administration. Ring-enhancing tuberculomas are usually 1 cm or less in size.[10] In severe tuberculous meningitis, the possibility of basal ganglia infarction, and / or communicating hydrocephalus should be actively investigated.[10] The classic basal meningeal enhancement can be well appreciated in sagittal post-contrast T1W images (Figure 5). Tuberculomas can be distinguished from tuberculous abscess, in which MRI shows a much larger and frequently multiloculated granuloma with central liquefaction and surrounding oedema.[10]

Degenerative Diseases

There are certain degenerative processes that involve the brain, and sagittal MRI of the brain provides an excellent diagnostic plane to view these processes. One of these neurodegenerative disorders, progressive supranuclear palsy, is characterised by supranuclear ophthalmoplegia, neck dystonia, postural instability, and mild dementia. The early stages of progressive supranuclear palsy are difficult to detect in most imaging modalities. However, in the late stages, atrophy of the midbrain is seen with cisternal and ventricular dilatation, as there is thinning of the quadrigeminal plate with dilatation of the third ventricle; this is best seen in sagittal plane MRI (Figure 6). The pons retains its normal volume.[11]

Cerebellar atrophy is caused by many diseases that affect the brain such as metabolic disorders, stroke, and major depressive disorder. Clinical history is often more important in making the diagnosis than MRI findings alone. Phenytoin induces cerebellar damage and may interfere with intestinal absorption of folate, causing folate deficiency which, in turn, causes cerebellar atrophy (Figure 7). Seizures can cause cerebellar atrophy, as the cerebellum is sensitive to hypoxia. Chronic alcoholism is another notable aetiology of a neurodegenerative disorder.[12] On sagittal T1W or T2W images, there is diffuse cerebellar atrophy with normal orientation of the middle cerebellar peduncle and transverse pontine fibres, and preservation of the volume of the pons. This differentiates diffuse

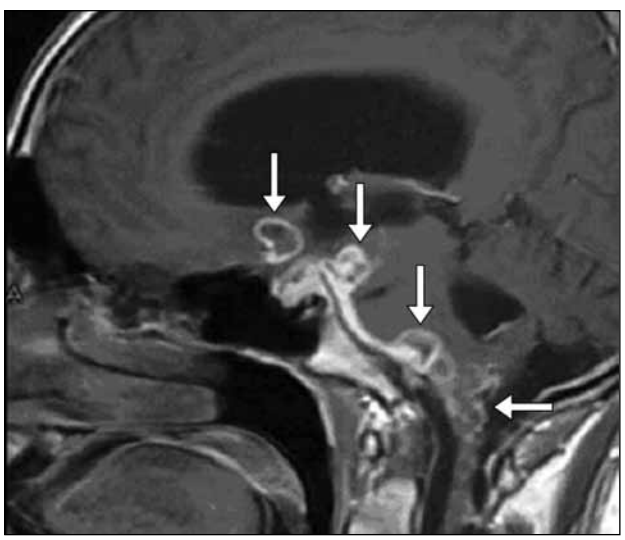

Figure 5. A sagittal plane post-contrast T1-weighted magnetic resonance image of the brain of a 26-year-old man with a history of treated pulmonary tuberculosis who presented with chronic headaches. The image shows pachy basal meningitis (horizontal arrow) along the anterior brain stem and multiple tuberculoma (vertical arrows).

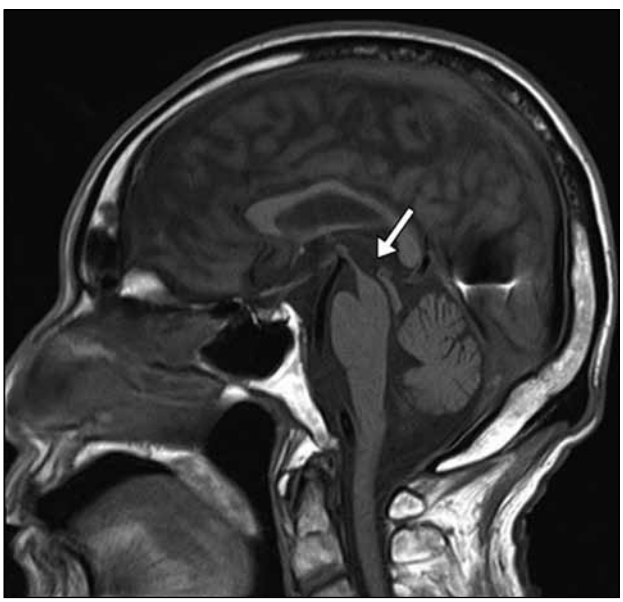

Figure 6. A sagittal plane T1-weighted magnetic resonance image of the brain of a 60-year-old man with loss of balance and frequent falls, inability to control eye movements, and muscle rigidity. The image shows the classic 'penguin' or 'humming bird' sign of progressive supranuclear palsy. There is thinning of the midbrain with atrophy of the tectum (arrow); the pons appears normal.

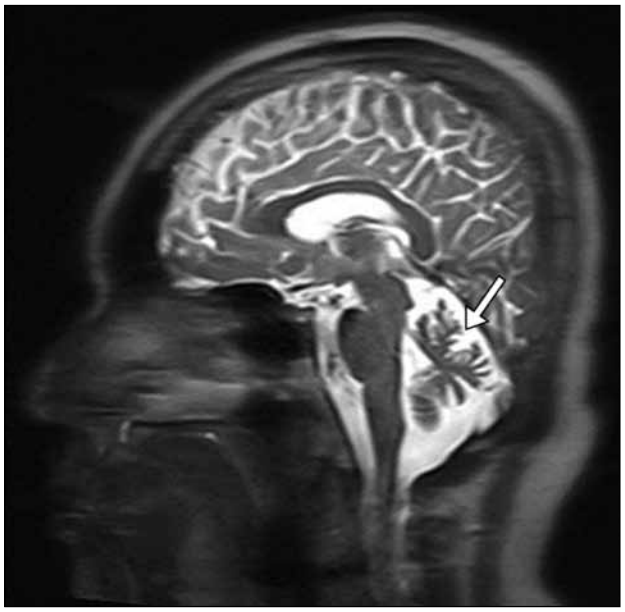

Figure 7. A sagittal plane T2-weighted magnetic resonance image of the brain of a 36-year-old man taking phenytoin long term who presents with gait instability and poor coordination. The image shows generalised cerebellar atrophy, with prominent folia and subarachnoid spaces (arrow); the pons is normal.

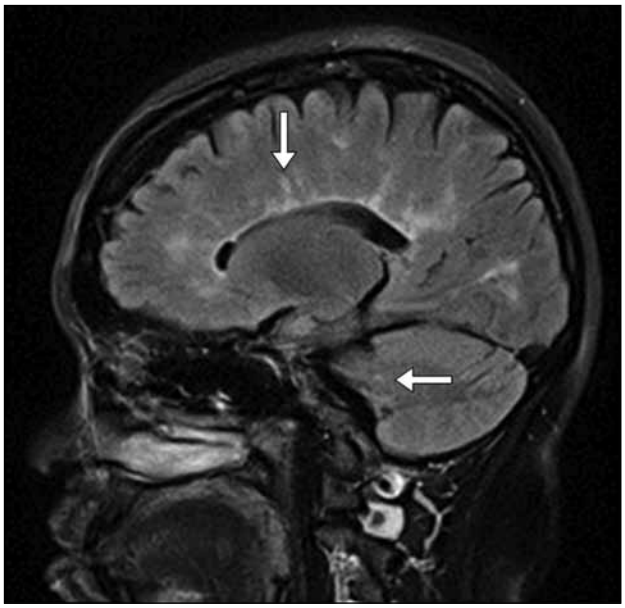

Figure 8. A sagittal plane fluid-attenuated inversion recovery magnetic resonance image of the brain of a 35-year-old woman with a history of lower limb numbness and lack of coordination. The paramidline plane shows discrete finger-like foci of abnormal signal intensities, or classic Dawson fingers (vertical arrow), extending into the periventricular white matter and brachium pontis (horizontal arrow). The imaging findings, together with clinical symptoms, support a diagnosis of multiple sclerosis.

cerebellar atrophy from other degenerative disorders such as multiple system atrophy.[12]

Demyelinating Disease

Multiple sclerosis is the most common inflammatory demyelinating disease of the CNS in young and middle-aged adults, but the condition also affects older people. Typically, the demyelinating plaques involve the corpus callosum, U fibres, temporal lobes, brainstem, optic chiasm, cerebellum, and spinal cord. This pattern of involvement is uncommon in other diseases. Sagittal plane T2W or fluid-attenuated inversion recovery MRI typically shows multiple perpendicular callosal septal T2W hyperintensities, characteristically known as Dawson fingers (Figure 8). Enhancing lesions suggest active demyelination.[13]

Neoplasms

Pituitary adenoma is classified as grade I in the World Health Organization grading system of intracranial tumours.[14] Sagittal plane MRI shows a sellar mass without an identifiable pituitary gland. Suprasellar extension is common in larger lesions (Figure 9).[15] Intratumoural haemorrhage is also known as pituitary apoplexy, and can be identified by hyperintense areas in sagittal plane T1W images. Pituitary microadenomas

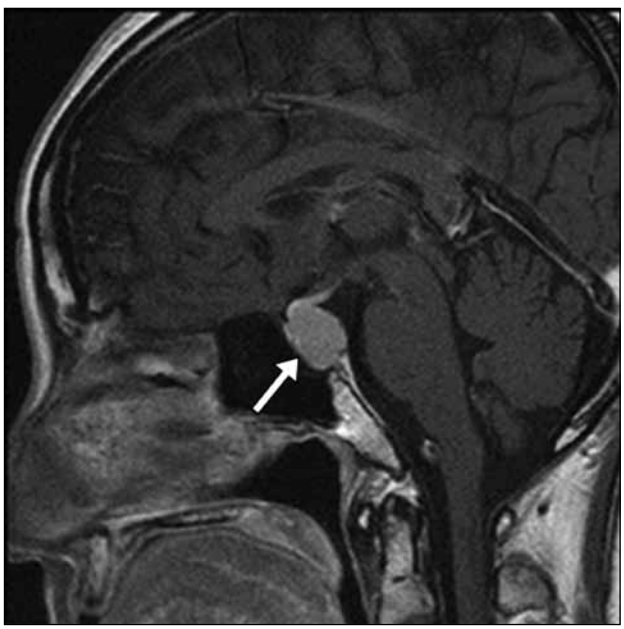

Figure 9. A sagittal plane post-contrast T1-weighted magnetic resonance image of the brain of a 40-year-old man with gynaecomastia and markedly elevated prolactin. The image shows a homogenously enhancing pituitary macroadenoma (arrow) resulting in expansion of the sella with suprasellar extension.

and the pituitary stalk can be best visualised on high-resolution dynamic-contrast MRI in the sagittal plane, in which most microadenomas appear as relatively non-enhancing lesions within an intensely enhancing pituitary gland in the arterial phase.[16]

Hamartoma of the hypothalamus and tuber cinereum represents a midline dysraphic syndrome, and presents as ectopic cerebral grey matter comprising a mass of normal neuronal tissue. Commonly, hamartomas are pedunculated and attached to the ventral surface of the hypothalamus anywhere from the tuber cinereum to the mammillary bodies by a distinct, thin or thick, stalk.[17] The typical sagittal plane MRI findings of hamartoma of the tuber cinereum is a well-circumscribed non-enhancing, iso- to slightly hyperintense to grey matter, lesion projecting into the post-chiasmatic, interpeduncular, and pre-pontine cistern regions (Figure 10).

Craniopharyngioma is a benign, often partially cystic, sellar region tumour derived from Rathke's pouch epithelium. This tumour has a bimodal age distribution with a peak at 5 to 15 years or older than 50 years.[18] On sagittal plane MRI, 75% of craniopharyngiomas are suprasellar, and often extend into multiple cranial fossae. The MRI signal of craniopharyngioma varies, with cyst contents and solid components showing heterogeneous enhancement (Figure 11).

Tumours of the pineal region account for about 1% of all brain tumours. MRI is necessary to view the relationship of the tumour with the surrounding brain structures in order to decide on the management plan.[19] Sagittal plane imaging shows typically heterogeneous masses involving the pineal gland and adjacent structures (Figure 12).

Histiocytosis is proliferation of Langerhans' cell histiocytosis, forming granulomas within any organ system. About 50% of histiocytoses involve the pituitary stalk, leading to diabetes insipidus.[20] Histiocytosis may be seen as the sole involvement of the CNS or as part of multisystemic involvement, such as in Hand-Schuller-Christian disease. On sagittal plane MRI, the brain shows an enhancing thick pituitary stalk or hypothalamic enhancing mass (Figure 13).

Rathke's cleft cysts are thought to arise from failure of obliteration of the lumen of Rathke's pouch.[21] In

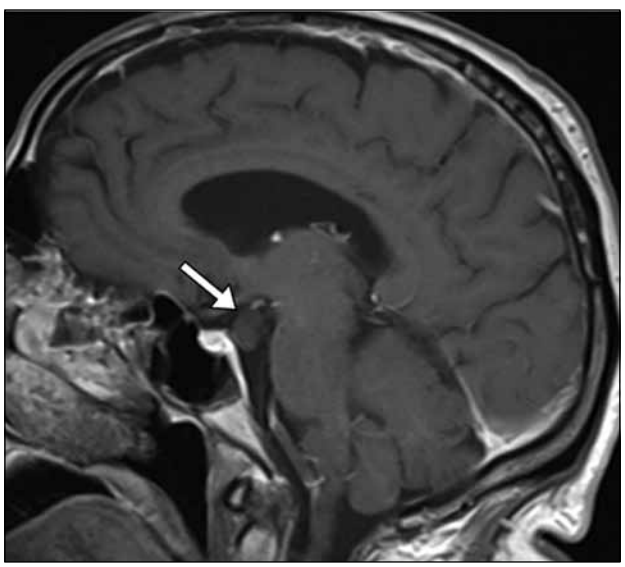

Figure 10. A sagittal plane T1-weighted magnetic resonance image of the brain of a 12-year-old girl with characteristic gelastic epilepsy. The image shows a small hypothalamic lesion (arrow), arising from the inferomedial hypothalamus, without any discernible enhancement, with features in keeping with a hamartoma of the tuber cinereum.

Figure 11. A sagittal plane post-contrast T1-weighted magnetic resonance image of the brain of a 15-year-old girl with worsening headaches and progressive bitemporal hemianopia for 4 months. The image shows a heterogeneous mass in the sellar and suprasellar region with a large T1-weighted hyperintense suprasellar component. The histopathology findings were compatible with craniopharyngioma.

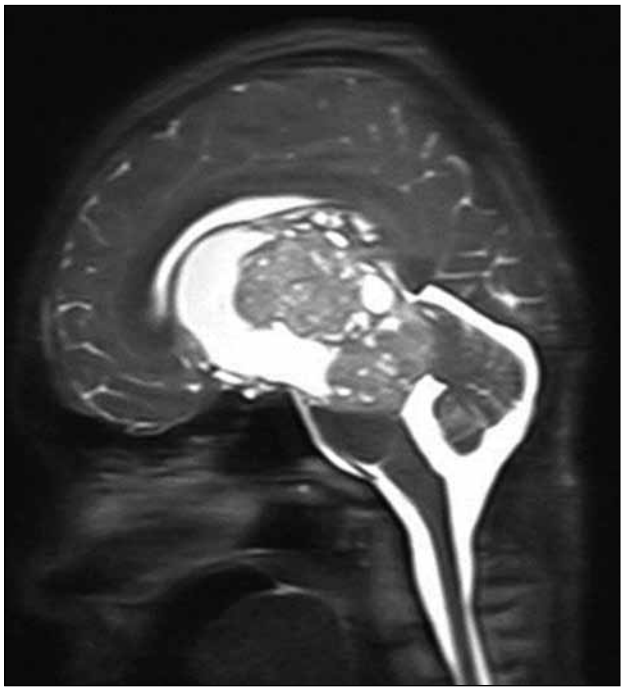

Figure 12. A sagittal plane T2-weighted magnetic resonance image of the brain of a 16-year-old man with headache and aggressive behaviour. The image shows a large heterogeneous mass involving the pineal tectum and thalami. The histopathological findings are compatible with pineocytoma.

Figure 13. A sagittal plane post-contrast T1-weighted magnetic resonance image of the brain of a 26-year-old woman with headache and diabetes insipidus. The image shows an enhancing mass involving the thickened pituitary stalk (arrow). The histopathological findings are compatible with histiocytosis.

sagittal plane MRI, the signal varies according to the cyst contents. There is often no central enhancement, although mild rim enhancement may be appreciated (Figure 14).

Vascular Abnormalities

Superior sagittal sinus thrombosis is the most common type of dural venous thrombosis and is potentially devastating. As with all cerebral venous thromboses, the presentation is highly variable, ranging from completely asymptomatic to a rapid fulminant course with cerebral haemorrhage and death. The presentation often includes sudden onset of severe headache.[22] The MRI features are the same as those of other dural sinus thromboses. An acute clot is isointense on T1W and hypointense on T2W images (this can mimic a flow void), with a sub-acute clot becoming hyperintense on T1W images (Figure 15). In addition, superior sagittal sinus thrombosis can be visualised by using phase-contrast magnetic resonance venography (MRV), in which the lack of flow and occlusion are seen on the reconstructed MRV maximal intensity projection images.[23]

Vein of Galen malformation (VGM) represents 1% of all vascular brain malformations. VGM develops from

Figure 14. A sagittal plane T2-weighted magnetic resonance image of the brain of a 20-year-old woman undergoing investigation of hypopituitarism. The image shows a very large combined intra- and suprasellar cystic mass (arrow). A Rathke's cleft cyst is found at operation.

Figure 15. A sagittal plane post-contrast T1-weighted magnetic resonance image of the brain of a 6-year-old boy with a hypercoagulable state presenting with severe headache. The image shows a long-segment filling defect in the superior sagittal sinus (arrow) compatible with superior sagittal sinus thrombosis.

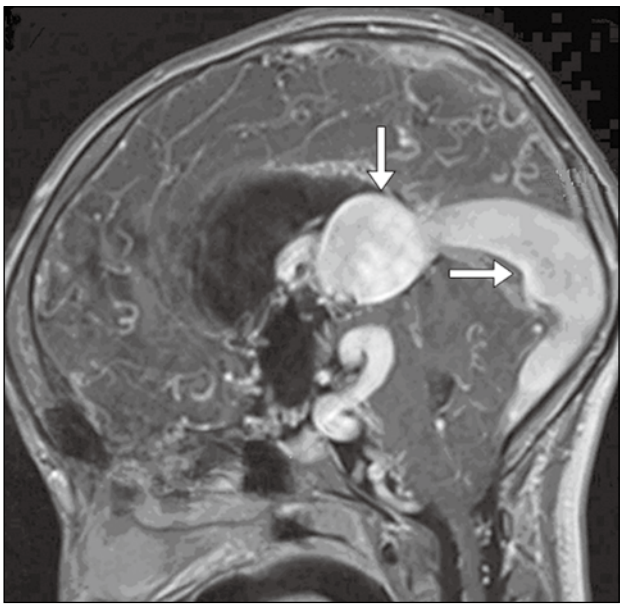

Figure 16. A sagittal plane post-contrast T1-weighted magnetic resonance image of the brain of a 2-year-old girl with congestive heart failure, in whom prenatal ultrasound showed multiple tortuous intracranial vessels. The image shows an enlarged median prosencephalic vein characteristic of vein of Galen arteriovenous malformation (vertical arrow) continuing in the falcine sinus (horizontal arrow), with enlarged confluence of sinuses. Arterial feeders can be seen along the anterior wall of the vein.

an arteriovenous fistula between the primitive choroidal vessels and the median prosencephalic vein.[24,25] Sagittal plane MRI easily demonstrates the median prosencephalic vein draining into the sagittal sinus, usually via a persistent falcine vein, and the straight sinus is absent (Figure 16).

CONCLUSION

Sagittal plane MRI provides a valuable 'one side of the story' for MRI diagnosis of different brain pathologies. Although the axial plane is most often used because of its ability to portray symmetrical structures and ease of detecting brain abnormalities, the sagittal plane is often included in brain imaging protocols because this imaging plane is useful on its own for providing diagnostic information about the different pathologies. This pictorial review has demonstrated the value of using the sagittal plane to provide a time-efficient method of reviewing pertinent findings on MRI.

DECLARATION

No conflicts of interests were declared by the authors.

REFERENCES

1. Ryan S, McNicholas M, Eustace SJ. Anatomy for diagnostic imaging. 2nd ed. Edinburgh: Saunders; 2004.
2. Yousefi B. Brain commissural anomalies. In: Mantamadiotis T, editor. When things go wrong — diseases and disorders of the human brain. Croatia: Intech Open Books; 2012. Available from: http://www.intechopen.com/books/when-things-go-wrong-diseases-and-disorders-of-the-human-brain/brain-commissural-abnormalities. Accessed 9 Oct 2013.
3. Harnsberger HR, Koch BL, Phillips CD, Glastonbury CM, Mosier K, Michel M, et al. Expertddx: head and neck. Philadelphia: Lippincott Williams & Wilkins; 2009.
4. Dähnert W. Radiology review manual. 6th ed. Philadelphia: Lippincott Williams & Wilkins; 2007.
5. Stevenson KL. Chiari Type II malformation: past, present, and future. Neurosurg Focus. 2004;16:E5. cross ref
6. Tisell M. How should primary aqueductal stenosis in adults be treated? A review. Acta Neurol Scand. 2005;111:145-53. cross ref
7. Stoquart-El Sankari S, Lehmann P, Gondry-Jouet, Fichten A, Godefroy O, Meyer ME, et al. Phase-contrast MR imaging support for the diagnosis of aqueductal stenosis. AJNR Am J Neuroradiol. 2009;30:209-14. cross ref
8. Gean-Manton AD, Vezina LG, Marion KI, Stimac GK, Peyster RG, Taveras JM, et al. Abnormal corpus callosum: a sensitive and specific indicator of multiple sclerosis. Radiology. 1991;180:215-21.
9. Maher D, Raviglione M. Global epidemiology of tuberculosis. Clin Chest Med. 2005;26:167-82,v. cross ref
10. Bernaerts A, Vanhoenacker FM, Parizel PM, Van Goethem JW, Van Altena R, Laridon A, et al. Tuberculosis of the central nervous system: overview of neuroradiological findings. Eur Radiol. 2003;13:1876-90. cross ref
11. Borroni B, Malinverno M, Gardoni F, Alberici A, Parnetti L, Premi

E, et al. Tau forms in CSF as a reliable biomarker for progressive supranuclear palsy. Neurology. 2008;71:1796-803. cross ref
12. Ney GC, Lantos G, Barr WB, Schaul N. Cerebellar atrophy in patients with long-term phenytoin exposure and epilepsy. Arch Neurol. 1994;51:767-71. cross ref
13. Calabrese M, Rocca MA, Atzori M, Mattisi I, Bernardi V, Favaretto A, et al. Cortical lesions in primary progressive multiple sclerosis: a 2-year longitudinal MR study. Neurology. 2009;72:1330-6. cross ref
14. Louis DN, Ohgaki H, Wiestler OD, Cavenee WK, Burger PC, Jouvet A, et al. The 2007 WHO classification of tumours of the central nervous system. Acta Neuropathol. 2007;114:97-109. cross ref
15. Kitajima M, Hirai T, Katsuragawa S, Okuda T, Fukuoka H, Sasao A, et al. Differentiation of common large sellar-suprasellar masses: effect of artificial neural network on radiologists' diagnosis performance. Acad Radiol. 2009;16:313-20. cross ref
16. Chaudhary V, Bano S. Imaging of the pituitary: recent advances. Indian J Endocrinol Metab. 2011;15(Suppl 3):S216-23. cross ref
17. Arita K, Ikawa F, Kurisu K, Sumida M, Harada K, Uozumi T, et al. The relationship between magnetic resonance imaging findings and clinical manifestations of hypothalamic hamartoma. J Neurosurg. 1999;91:212-20. cross ref
18. Boongird A, Laothamatas J, Larbcharoensub N, Phudhichareonrat S. Malignant craniopharyngioma: case report and review of the literature. Neuropathology. 2009;29:591-6. cross ref
19. Baehring J, Vives K, Duncan C, Piepmeier J, Bannykyh S. Tumors of the posterior third ventricle and pineal region: ependymoma and germinoma. J Neurooncol. 2004;70:273-4. cross ref
20. Marchand I, Barkaoui MA, Garel C, Polak M, Donadieu J; Writing Committee. Central diabetes insipidus as the inaugural manifestation of Langerhans cell histiocytosis: natural history and medical evaluation of 26 children and adolescents. J Clin Endocrinol Metab. 2011;96:E1352-60. cross ref
21. Byun WM, Kim OL, Kim D. MR imaging findings of Rathke's cleft cysts: significance of intracystic nodules. AJNR Am J Neuroradiol. 2000;21:485-8.
22. Larson TC III. Cerebral aneurysms and cerebrovascular malformations. In: Haaga JR, editor. CT and MRI of the whole body. 5th ed. Philadelphia: Mosby Elsevier; 2009. p 280-4. cross ref
23. Meckel S, Reisinger C, Bremerich J, Damm D, Wolbers M, Engelter S, et al. Cerebral venous thrombosis: diagnostic accuracy of combined, dynamic and static, contrast-enhanced 4D MR venography. AJNR Am J Neuroradiol. 2010;31:527-35. cross ref
24. Jones BV, Ball WS, Tomsick TA, Millard J, Crone KR. Vein of Galen aneurysmal malformation: diagnosis and treatment of 13 children with extended clinical follow-up. AJNR Am J Neuroradiol. 2002;23:1717-24.
25. Lee EJ. The empty delta sign. Radiology. 2002;224:788-9. cross ref